AIMS Biophysics

AIMS Biophysics, 13(1): 80−93.
DOI: 10.3934/biophy.2026005
Received: 12 November 2025
Revised: 12 February 2026
Accepted: 24 February 2026
Published: 16 March 2026

http://www.aimspress.com/journal/biophysics

Research article

Localization of the inner body in jumbo phage phiK601 by Cryo-EM and high-dose imaging

Andrey V. Moiseenko[1], Ishika Gupta[2], Grigorii Mitrov[1], Mikhail Egorochkin[1], Ruqaiyah Khan[2], Virajith Boddapati[2], Sayani Das[2], Sandip Kaledhonkar[2], Kiran Kondabagil[2,3,*] and Olga S. Sokolova[1,4,5,*]

[1] Faculty of Biology, Lomonosov Moscow State University, Moscow, 119234, Russia
[2] Department of Biosciences and Bioengineering, Indian Institute of Technology Bombay, Mumbai, 400076, India
[3] Koita Centre for Digital Health (KCDH), Indian Institute of Technology Bombay, Mumbai, 400076, India
[4] Faculty of Biology, Shenzhen MSU-BIT University, Shenzhen, 518172, China
[5] Key Laboratory of Forest Plant Ecology, Ministry of Education, Northeast Forestry University, Harbin, 150040, China

* **Correspondence:** Email: sokolova@mail.bio.msu.ru, kirankondabagil@iitb.ac.in; Tel: +13603017074, Tel: +918025767758.

Abstract: Jumbo bacteriophages possess exceptionally large capsids accommodating genomes that encode additional proteins, which support their infection and replication. A distinctive structural element, known as the inner body, has been observed in a number of phiKZ-like phage particles and its proteins are believed to play an essential role in phage genome organization and ejection. However, the precise localization and three-dimensional structure of the inner body have remained elusive. Here, we applied the high-dose cryo-electron microscopy ("bubblegram") approach to localize the inner body within the capsid of phiKZ-like jumbo phage phiK601. The inner body was resolved as a cylindrical structure approximately 22 nm in diameter, tilted by ~ 20° relative to the tail axis and positioned asymmetrically, likely contacting the portal vertex and the opposing capsid edge. It is surrounded by 17 concentric layers of packaged DNA and exhibits positional flexibility within the capsid.

Keywords: jumbo phage; cryo-electron microscopy; inner body; bubblegrams; phiK601

1. Introduction

Jumbo phages are a distinct group of bacteriophages that possess exceptionally large genomes, exceeding 200 kb of double-stranded DNA [1,2]. Such expanded genomes enable jumbo phages to encode many genes absent in smaller phages, resulting in greater functional complexity and self-reliance. These include chimallin [3], PhuZ [4], and the inner body proteins [5]. In addition to encoding proteins, jumbo phages can package proteins within their capsids [6]. For example, the *Pseudomonas aeruginosa* phiKZ phage carries a viral RNA polymerase (vRNAP) [7,8], making phage independent from host cellular machinery [9]. The larger the genome, the larger the capsid is required to accommodate it [10]. To package the extended DNA and associated proteins, jumbo phage capsids reach dimensions of up to ~ 1600 Å [11,12]. However, as demonstrated in [13,14], the average DNA density within jumbo phage capsids can vary considerably, with the lowest densities observed in the largest capsids, such as those of PBS1 and phage G, thereby providing additional space for the packaging of proteins. In the case of phage G, the DNA is packed so loosely that it does not even form the typical concentric layers usually observed by cryo-EM [15].

The unique proteinaceous feature termed the inner body (IB) is inside the capsids of phiKZ-like phages, first identified with electron microscopy [16]. The IB appears as a rod-like density, spanning the capsid interior from wall to wall [5,12,16–18] and is thought to play an important role in the regulation of genome packaging. One proposed role is that of a proteinaceous rod-like scaffold that spools DNA around itself during capsid filling [5,17,19,20]. The IB has also been suggested to act as a reservoir for proteins destined to be ejected during infection [21,22]. Consistent with this idea, electron microscopy has shown that the IB is absent from capsids after DNA release, indicating that it is co-ejected with the genome [16].

Biochemical and mass spectrometry analyses have shown that several capsid proteins contribute to IB formation, with six proteins, gp89, gp90, gp93, gp95, gp97, and gp162, being the most abundant. Each is present in more than 100 copies per virion, yielding a total IB mass of ~ 15−20 MDa [5,23]. All these phiKZ proteins undergo proteolytic cleavage during maturation by the same protease, gp175 [23], which recognizes the conserved cleavage motif S/A/G-X-E. Additional proteins, such as gp94 and gp163, are also processed by this protease [24]. Despite differences in precursor size, the mature products share structural similarities. For example, gp93, gp95, and gp162 each contain the paralogous domain PF12699, which is also found in gp94 and gp163 [5]. Generally, propeptides are acidic, whereas their mature products are neutral or slightly positively charged, consistent with a possible role in DNA binding. Given the high abundance of IB-related proteins and the occurrence of two cleavages per some of them, the maturation of a single phiKZ capsid involves more than six proteolytic cleavages [24]. While some resulting fragments may be non-functional debris (e.g., the short N-terminal fragment of gp89), the functional role of most IB proteolytic products remain unclear.

Using cryo-EM approaches IB-like densities have been visualized in *Pseudomonas* phiKZ-like phages phiKZ, EL, Lin68, 201phi2-1 [5,17,18]. In contrast, other jumbo phages, including Phage G, PAU, PBS1, and phiN3, appear to lack inner bodies [13,15]. These observations suggest that jumbo phages employ at least two distinct strategies for organizing their genomic DNA: One involving an inner body scaffold, and one without it [14]. There is only minor evidence of IB-like rod feature in *E.*

coli phage 121Q and *R. solanacearum* RSL2 [13,14], but in both cases, the cryo-electron microscopy data may be interpreted ambiguously. A low-resolution reconstruction of PhiKZ phage's IB was obtained more than a decade ago [17,18]. However, no high-resolution structural data are available for the IB. One of the major challenges in reconstructing the IB arises from its location beneath the highly compacted DNA inside the capsid. DNA and capsid shell proteins strongly scatter electrons and dominate during particle projection alignments, while the weaker signal of the IB is effectively lost during three-dimensional reconstruction.

A specialized high-dose cryo-EM approach, known as "bubblegrams", was suggested about a decade ago to reveal the inner body and other proteins inside the phage capsids [17,18,25,26]. In conventional cryo-EM experiments, the electron dose is kept below 50–60 $e^{-}/Å^{2}$; in combination with subsequent dose-weighting of images, this minimizes the effects of radiation damage on the resolution. At higher doses, however, radiation damage accumulates, leading to sample degradation. One sign of this damage is the formation of hydrogen bubbles, caused by water radiolysis [27]. Proteins embedded within the highly compacted DNA appear to be more susceptible to bubbling than either free-standing proteins or DNA origami [28]. The bubblegram imaging of bacteriophage T7 and P22 [25,26] revealed the structures of massive core and portal proteins, which was consistent with the high resolution cryoEM structures published later [29–31].

In this work, we employed an image collecting approach, based on obtaining extended movies corresponding to a total dose of 140 $e^{-}/Å^{2}$, and used the information from high and low dose frames to align particle projections. We built a three-dimensional reconstruction of a capsid of phiKZ-like jumbo phage phiK601, which showed the asymmetric positioning of the inner body within the capsid. We anticipate that this approach will be useful in future cryo-EM studies of inner proteinous structures in other phages.

2. Materials and methods

2.1. Genome sequencing

Genomic DNA was isolated from the purified phiK601 suspension using a Qiagen DNA extraction kit (Qiagen N.V., Germany) according to the manufacturer's instructions. Sequencing was carried out at MedGenome Labs Ltd. (Bengaluru, India) using the Illumina NovaSeq sequencing platform. Library preparation and sequencing were performed following standard Illumina protocols to generate paired-end reads. The raw sequence reads were subjected to quality control, including adapter removal, trimming of low-quality bases, and filtering of short reads. High-quality reads were assembled de novo using the SPAdes assembler (v3.11.1) to generate contiguous sequences. The assembled genome was subsequently annotated using Prokka, which predicted coding DNA sequences (CDSs), genes, and other genomic features.

2.2. Isolation and purification of phiK601 for cryo-EM data collection

The bacteriophage phiK601 was isolated (June 22, 2022) from a water sample collected from Powai Lake, Mumbai, India [19.1273° N, 72.9048° E]. The water sample was centrifuged at 12,000 *g* for 5 min to remove particulate matter, and the supernatant was filtered through a 0.45 μm membrane filter. For phage enrichment, 1% (v/v) of an overnight *P. aeruginosa* PAO1 culture was inoculated into

a mixture of Luria-Bertani (LB) broth and filtered lake water (1: 1, v/v) and incubated at 37 °C with shaking. Following enrichment, the culture was centrifuged at 12,000 *g* for 10 min to remove bacterial debris, and the supernatant was again filtered through a 0.45 μm membrane. The presence of lytic phages was confirmed using the double-layer agar plaque assay. A single plaque was picked using a sterile tip and resuspended in 10 μl of SM buffer [100 mM NaCl, 8 mM $MgSO_4$, 50 mM Tris-HCl, 0.01% gelatin, pH 7.5]. The phage was purified through five rounds of single-plaque isolation to ensure clonality. The purified phage phiK601 produced clear, small plaques on the PAO1 lawn and was selected for further characterization.

A single colony of PAO1 was inoculated into 5 mL of LB medium and incubated overnight at 37 °C with shaking at 150 rpm. The overnight culture (1% v/v) was used to inoculate 500 mL LB in a 2 L flask and grown at 37 °C until the optical density at 600 nm reached 0.3−0.5. Phage phiK601 was then added at an MOI of 1, and the culture was incubated for 8 hrs with shaking until complete lysis was observed. Following lysis, chloroform (5−10 mL) was added and incubated for 10 min with shaking to ensure complete cell lysis, followed by treatment with DNase I and RNase A to a final concentration of 1 μg/mL and incubation for 30 min at room temperature.

The DNase I and RNase A treated lysate was clarified by centrifugation at 10000 *g* for 10 min at 4 °C to remove cell debris and chloroform. NaCl was added to a final concentration of 1 M and the supernatant was incubated on ice for 2 hrs. It was then mixed with polyethylene glycol (PEG 8000) to a final concentration of 10% (w/v) to precipitate the phage particles. The precipitate was collected by centrifugation at 13,000 *g* for 20 min at 4 °C, and the pellet was drained and resuspended in SM buffer (10 mL per 500 mL culture) and incubated at room temperature for 1 hr. Residual PEG and cell debris were removed by further chloroform extraction. An equal volume of chloroform was added to the phage suspension, mixed gently, and centrifuged at 10,000 × *g* for 15 min to separate the organic and aqueous phases. The aqueous phase was carefully collected without disturbing the interphase, and the extraction was repeated twice to ensure purity.

The phage suspension was layered onto a CsCl step-gradient ultracentrifugation (1.6, 1.5, 1.4, 1.3, and 1.2 g/mL CsCl layers) and centrifuged at 108,000 *g* for 3 hrs at 4 °C in the SW41 Ti rotor (Beckman Coulter). Intact phage particles formed a distinct bluish band at approximately 1.45 g/mL, which was carefully collected and dialyzed twice against 1 L of gelatin-free SM buffer (first containing 1 M NaCl, then without NaCl) to remove CsCl.

2.3. Cryo-electron microscopy

The grids were prepared using Quantifoil R1.2/1.3 with an additional 2 nm carbon layer. Glow discharge was performed for 120 sec at 20 mA under surface-negative and air-positive conditions to enhance the hydrophilicity of the grids with Quorum GloQube Plus. Samples were prepared in the Vitrobot Mark IV system (ThermoFisher Scientific). After the sample application, grids were incubated for 30 sec before blotting for 3 sec with a blot force of 0 in controlled humidity conditions. Immediately after blotting, grids were plunge-frozen in liquid ethane to preserve sample integrity for subsequent imaging.

Cryo-electron microscopy data were collected using a Thermo Fisher Scientific Titan Krios G4 microscope operated at an accelerating voltage of 300 kV and equipped with a Gatan K3 BioContinuum direct electron detector with an energy width of 20 eV. Images were recorded in super-resolution mode at a nominal magnification of 42,000x, corresponding to a calibrated pixel size of

1.06 Å. A total of 2,929 movies were acquired, each comprising 100 frames with a total accumulated exposure of 140 e^{-}/Å² and average defocus of minus one micrometer.

2.4. Data processing

Single-particle data processing (Figure 1) was performed in the cryoSPARC software [32]. For initial processing, dose-weighted patch motion correction was applied only to the first 40 frames of each movie (corresponding to a cumulative dose of 56 e^{-}/Å²), followed by patch CTF estimation for the corrected micrographs. Virion capsids were picked using a blob picker with a circular template diameter of 1,400–1,800 Å. After the removal of false-positive picks by 2D classification, 3,593 particles were retained for further analysis. An initial 3D reconstruction was generated *de novo* using the *ab initio* algorithm and refined by homogeneous refinement under icosahedral symmetry, yielding a consensus map at 8.1 Å resolution.

Particles with assigned orientations were then re-extracted from dose-weighted micrographs generated using only the final 30 frames of each movie (corresponding to a total dose of 140 e^{-}/Å²). A 3D reconstruction obtained without additional alignment reached a resolution of ~ 30 Å. Attempts to improve this map by further 3D refinement were unsuccessful.

Using the 3D density map and particle orientations, we performed particle subtraction to remove the capsid shell density. The dataset was then symmetry-expanded according to icosahedral symmetry, followed by 3D classification without particle realignment. A spherical mask covering the capsid interior was used for classification, which revealed classes displaying a cylindrical density consistent with an inner body positioned asymmetrically within the capsid.

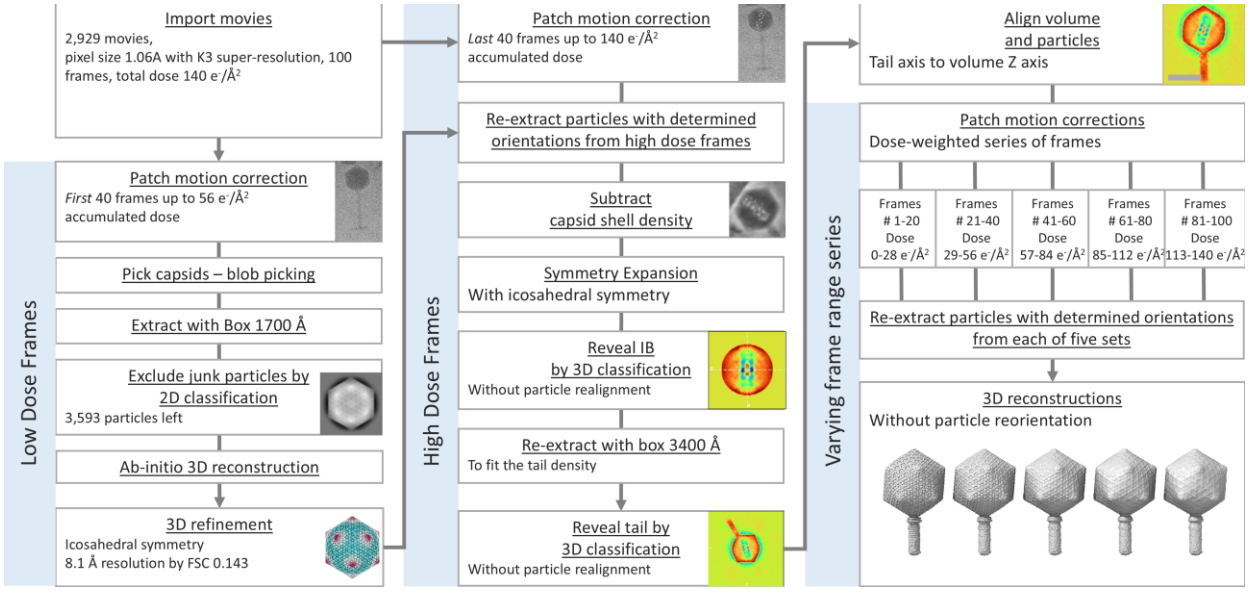

Figure 1. Cryo-electron microscopy data-processing workflow. The left column outlines the preprocessing steps and generation of the consensus icosahedrally averaged capsid reconstruction. The center column illustrates the re-extraction of the consensus particles from the high-dose frames subsequent the reconstruction of a 3D density map displaying the inner body and the phage tail. The right column shows the procedure for a series of reconstructions with an accumulating dose.

Particles from one such class were re-extracted with a larger box size to include both the capsid and a significant portion of the tail. In this case, no particle subtraction was performed. A cylindrical mask corresponding to the putative tail location relative to the capsid was created in ChimeraX [33] and applied during 3D classification. This procedure identified a subset of particles oriented such that the inner body cylinder and the tail density were simultaneously resolved in the 3D reconstruction. Duplicate particles generated by symmetry expansion were removed, and the final volume was reoriented with the tail axis aligned along the Z-axis.

A series of dose-weighted micrographs was generated by performing dose-weighted patch motion correction on five frame ranges: 1–20, 21–40, 41–60, 61–80, and 81–100, corresponding to cumulative electron doses of 28, 56, 84, 112, and 140 $e^{-}/Å^{2}$, respectively. Particles with previously assigned orientations were re-extracted from each dataset, and a separate 3D reconstruction was computed for each dose range without additional particle realignment. For all reconstructions, a 3D mask encompassing the capsid and the attached tail segment was applied during refinement.

3. Results

3.1. Capsid and inner body proteins of phiK601 are highly homologous to phiKZ

The phiK601 (GenBank accession ID: PV976809) genome indicates that it is a phiKZ-like bacteriophage belonging to the *Chimalliviridae* family (Figure 2). It possesses a large genome of approximately 280,452 base pairs, encoding 369 predicted genes with a GC content of around 36.81%. Comparative genomic analysis [34] with phiKZ (GenBank accession ID: AF399011; genome size of 280,334 base pairs) demonstrates a high degree of sequence similarity across extensive regions of their genomes, reinforcing their close evolutionary relationship and placing phiK601 within the phiKZ-like phage group. This close similarity also aligns with the conserved functional and structural features typical of jumbo phages within this family, highlighting phiK601 as a distinct but closely related strain in the phiKZ lineage.

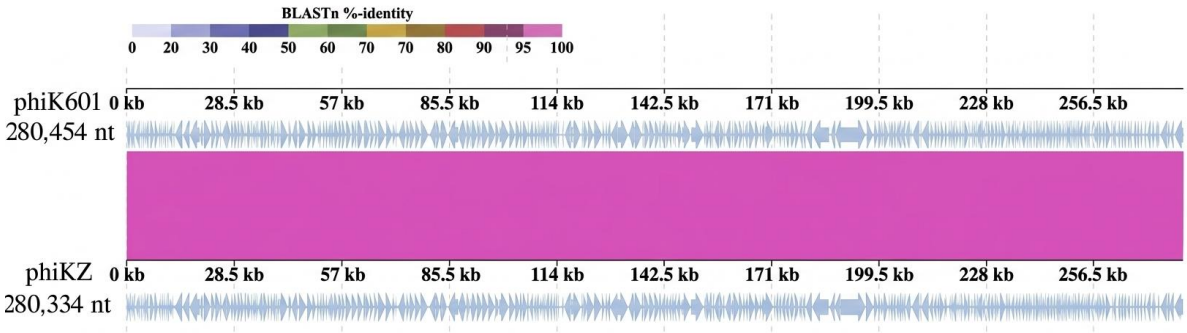

Figure 2. The whole genome comparison of bacteriophages phiK601 (280,452 bp) and phiKZ (280,334 bp) using DiGAlign. The panel shows a linear BLASTn alignment with colored shading, indicating the high sequence identity (> 95%) between the two jumbo phages. The predicted genes are represented above and below the alignment for phiK601 and phiKZ, respectively.

The gene products representing the capsid proteins share the sequence with the corresponding phiKZ proteins (Table 1).

Table 1. Capsid and inner body proteins of phiKZ and corresponding proteins of phiK601.

Functional/structural role	phiKZ gene product	phiK601 gene product	Sequence Identity, %
Minor capsid protein (inner)	gp28	HPCPLMGF_00032	99.6
Decorating protein (outer)	gp35	HPCPLMGF_00042	93.0
Minor capsid protein (inner)	gp85	HPCPLMGF_00107	96.4
Minor capsid protein (inner)	gp86	HPCPLMGF_00108	99.8
Inner body protein	gp89	HPCPLMGF_00111	100.0
Inner body protein	gp90	HPCPLMGF_00112	100.0
Minor capsid protein (inner)	gp91	HPCPLMGF_00113	100.0
Inner body protein, Minor capsid protein (inner)	gp93	HPCPLMGF_00115	97.0
Inner body protein	gp95	HPCPLMGF_00118	98.3
Inner body protein	gp97	HPCPLMGF_00120	97.9
Minor capsid protein (inner)	gp119	HPCPLMGF_00151	100.0
Major capsid protein	gp120	HPCPLMGF_00152	99.0
Inner body protein, Minor capsid protein (inner)	gp162	HPCPLMGF_00198	98.6
Minor capsid protein (inner)	gp184	HPCPLMGF_00224	95.6
Decorating protein (outer)	gp244	HPCPLMGF_00296	95.7

3.2. The bubbles revealing inner body appear during the electron dose accumulation

We performed cryo-electron microscopy analysis of the phiK601 virion heads and determined the IB 3D positioning inside the capsid. In standard cryo-EM data collection, the total accumulated electron dose is typically limited to ~ 40–60 $e^{-}/Å^{2}$ per field of view, with subsequent dose-weighting

during motion correction. In this study, we acquired extended movies reaching a total exposure of 140 $e^{-}/Å^2$. Using frames corresponding to a cumulative dose range of 0–42 $e^{-}/Å^2$, we reconstructed the 3D structure of the capsid at 8 Å resolution (Figure 3A). The resulting density map demonstrates that the diameter of the capsid is 1450 Å (T = 27) from vertex to vertex. This is identical to dimensions and T-triangulation symmetry of phiKZ-like phages [12,15], similar to ϕKp24 [7] phage, and larger than phiRSL1 phage (123 nm) [35]. Inspection of individual frames reveals the start of the formation of bubbles within the capsids of phiK601 (Figure 3B–D) at doses exceeding ~ 80 $e^{-}/Å^2$. These bubbles form a characteristic cylindrical pattern within the capsid, consistent with earlier high-dose observations of phiKZ [17,18].

Interestingly, the presence of minor decorating protein densities at the capsid vertices of phiK601 (Figure 3F) suggests that the capsid shell composition of phiK601 is similar to that of phiKZ [12].

The two-dimensional classification of two sets of particles extracted from frames with cumulative doses of 0–42 $e^{-}/Å^2$ and 98–140 $e^{-}/Å^2$ reveal that the inner body appears as a distinct cylindrical density spanning the capsid interior (Figure 3B, C). Notably, all particle projections displaying the inner body cylinder show it as a side view, but never as a top view, indicating that none of the inner body cylinders are oriented perpendicular to the ice plane. This observation implies that the inner body of phiK601 is aligned at a sharp angle relative to the tail axis of the phage.

We used high-dose frames (98–140 $e^{-}/Å^2$), which display a strong contrast from radiation-induced bubbles, to guide three-dimensional classifications and to isolate a subset of particles oriented in such a way that the resulting reconstruction contains the capsid shell, portal, tail, and inner body densities. By re-extracting particles with determined orientations from different frame ranges, we generated a series of 3D reconstructions depicting the progressive formation of bubbles (Figure 3D, E). Although radiation damage and capsid deformation prevent these high-dose particles from yielding high-resolution reconstructions, they nevertheless enable the visualization of the inner body's position relative to the capsid. Bubble formation becomes apparent at cumulative doses above approximately 80 $e^{-}/Å^2$.

Although high-dose bubblegrams span the length of the capsid, the low-dose reconstruction captures only a portion of IB. The IB density lacks any discernible features that can be interpreted as the tertiary protein structure. On side projections, a faint periodic pattern with a spacing of ~ 14 nm is visible (Figure 3F); however, given the absence of tertiary structure information, this feature should be interpreted with caution and may represent an artifact. The absence of discernible structural features in the inner body density suggests that it is positionally flexible rather than being rigidly fixed within the capsid, as suggested before [13], and may undergo rotational motion relative to the capsid shell or around its own axis. Accordingly, the reconstruction should be interpreted as revealing the position of the inner body within the capsid rather than its detailed molecular structure.

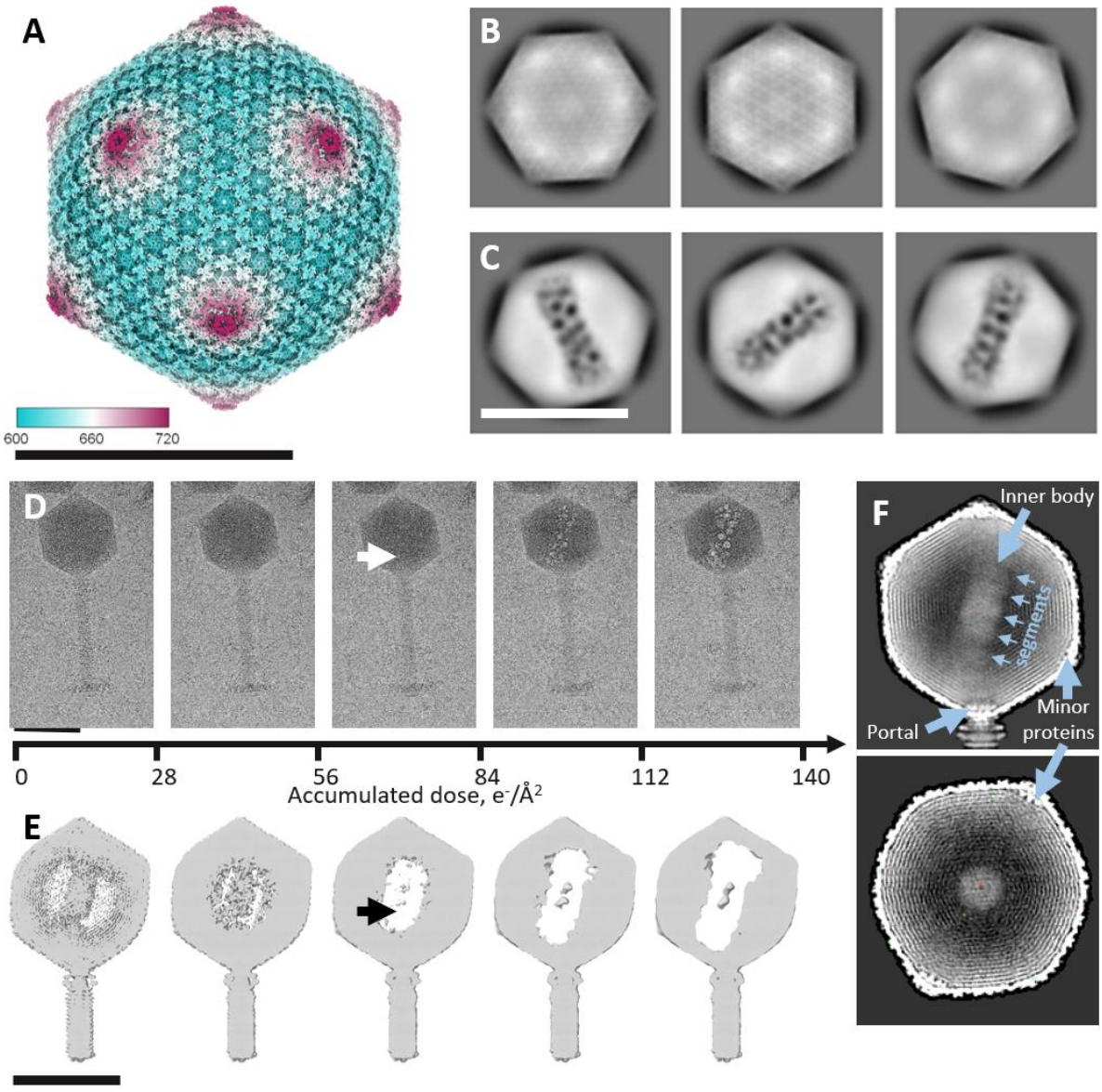

Figure 3. Cryo-electron microscopy reveals radiation-induced bubble formation within the inner body of the jumbo phage phiK601. (A) Three-dimensional reconstruction of a phiK601 virion capsid at 8.1 Å resolution. The density map is colored by radial distance from the capsid center. (B, C) Representative 2D class averages of phiK601 capsids imaged under low (B) and high (C) electron doses. (D) Series of images illustrating the progression of bubble formation with an increasing accumulated electron dose; the arrow marks the first sign of bubble formation. (E) Slices through 3D reconstructions showing the transformation of density corresponding to the inner body as a function of dose; arrow marks the weakened density for the inner body. The 2D images in (D) and the 3D reconstructions in (E) are generated from particle stacks corresponding to successive cumulative dose intervals, as indicated at the axis. (F) Slices through the asymmetric 3D density map taken parallel and perpendicular to the inner body cylinder. The contrast is inverted to enhance the visibility. Scale bar equals to 100 nm (all panels).

4. Discussion

PhiKZ is the first giant phage discovered more than 45 years ago [36]. It was characterized by a large genome size and a giant (comparable to standard phages) head and tail. Unexpectedly, upon experiments with tailless mutants of phage phiKZ, an extra structural part was observed inside the capsid: It had a compact structure and was visible only in damaged capsids [37]. It was named "the inner body" and was suggested to play a significant role in headful DNA packing, namely arranging genomic DNA inside a giant phage head [16,17].

For a long time, this feature had been suggested to be an artifact of sample preparation. Yet, multiple results obtained with different methods finally proved its existence. It was confirmed by atomic force microscopy after the DNAse treatment of phiKZ phages [38], visualized by bubblegram forming using high dose application [17,18]. The mass of the phiKZ IB was an estimated 15–20 MDa. Proteomic experiments on the tailless phiKZ mutant [5] revealed six internal proteins associated with the IB.

The available microscopy data demonstrated that a number of phiKZ-like phages possess IBs [5,17,18]. The IB is faintly visible in raw cryo-EM images of many phage heads. However, reconstructing its three-dimensional structure under low-dose conditions presents a major challenge, as the IB is embedded within the strongly scattering densities of the symmetric capsid shell and the compacted DNA. These dominant features guide the particle alignment during single-particle reconstruction, causing the asymmetric and lower signal-to-noise ratio of IB to be averaged. During this work, we applied conventional approaches to resolve symmetry-mismatched components in the capsid [39], but this did not yield a successful reconstruction of the IB (Figure 3A).

In this work we isolated the phiKZ-like bacteriophage phiK601 from a water sample collected from Powai Lake, Mumbai, India. Genome comparison shows that phi601 and phKZ share regions of high sequence identity, consistent with a close evolutionary relationship. The presence of the proteins that belong to the IB (Table 1) suggest that phi601 also possess this structural feature.

We obtained high-dose cryo-EM images with the frame range extended to 100 and corresponding total dose of 140 $e^{-}/Å^{2}$. We used high dose frames to align particles to an inner body density and then used low dose frames to obtain a low-resolution asymmetric reconstruction of the phiKZ-like phage phiK601 (Figure 3F). Inspection of the low-dose density map at 17 Å resolution revealed that the inner body forms a cylindrical structure approximately 22 nm in diameter, tilted by ~ 20° relative to the portal axis. Wu et al. [17] suggested that the IB of phiKZ is anchored on opposing hexons, on either side of the capsid, tilted at 22°. Here, we show that the IB of phiK601 is not anchored at the capsid vertices, but is positioned asymmetrically, extending from the vicinity of the portal complex toward one of the opposing icosahedral edges. The orientation of the cylinder, with one end directed toward the portal vertex, suggests a potential interaction between the inner body and the portal complex. The inner body is surrounded by 17 concentric layers of packaged DNA (Figure 3F).

Importantly, the capsids of jumbo phages contain sets of decorating proteins lining the inner capsid surface [12–14,35]. The functions of these proteins remain largely unknown, but they are thought to contribute to capsid stability and possibly facilitate capsid assembly. The high-resolution structure of the phiKZ capsid [12] revealed multiple protein complexes on the inner surface, including a vertex complex that bridges pentameric and hexameric capsomers, as well as a fiber-like network of minor proteins stabilizing the connections between capsomers. Not all jumbo phages, however, possess such additional proteins on the inner surface; yet, they can maintain large and stable capsids capable

of accommodating genomes of comparable length. So far, a few high-to-middle resolution capsid structures of jumbo phages have been published [11–14,35]. Nevertheless, they suggest that jumbo phages employ at least two distinct strategies for organizing their genomic DNA: One involving an IB scaffold, and one without IB.

5. Conclusions

Here, we suggested an original strategy that enabled us to exploit radiation-induced bubbles from protein encased with DNA generated under high electron doses, and to make a 3D reconstruction of the IB inside a giant phage capsid. The accumulated radiation dose causes a decay of high spatial frequencies, leading to image blurring that prevents the direct use of high-dose particles for 3D refinements. The same particles were then re-extracted from high-dose frames exhibiting strong bubble contrast and subjected to 3D classification without particle realignment, yielding a subset of particles whose reconstruction contained the IB, portal, and tail densities. Finally, we reverted back to particles from low-dose frames and generated a 3D reconstruction. This strategy enabled us to visualize the 3D position of the inner body inside the phiK601 virion. We anticipate that this approach will be useful in future cryo-EM studies of inner body structures in other phages, particularly those exhibiting lower structural heterogeneity.

Use of generative-AI tools declaration

The authors declare they have not used Artificial Intelligence (AI) tools in the creation of this article.

Acknowledgments

Authors thank Mrs Lisa Trifonova for proof-reading the manuscript. The cryo-EM reconstruction was supported by RSF (24-44-02003 to O.S.S.) and the phage isolation and purification−by Department of Science and Technology, India (DST/INT/RUS/RSF/P-79/2023 to K.K.). K.K. lab was also supported partly by funding from the Indian Council of Medical Research, ICMR (IIRPSG-2024-01-02611), and the Council of Scientific and Industrial Research (CSIR, 37/1752/23/EMR-II). S.K. lab acknowledges support from Science and Engineering Research Board, Government of India (IPA/2020/000413). We also thank the ANRF and IoE-supported national cryo-EM facility at IIT Bombay.), V.B. also acknowledges the fellowship from the Council of Scientific & Industrial Research (CSIR), India (Grant No: 09/0087(13984)/2022-EMR-I).

Conflict of interest

The authors declare no conflict of interest.

Author contributions

A.V.M. performed cryo-EM data processing and drafted the manuscript with input from all authors, M.E. and G.M. performed phage capsid reconstruction, I.G., R.K., and S.D. performed the

phage purification, genomics, and virology studies, G.M. performed partial annotation of head and inner body proteins, S.K. supervised the cryo-electron microscopy data collection, V.B. performed cryo-electron microscopy data collection, K.K. and O.S.S. designed and supervised the study.

References

1. Yuan Y, Gao M (2017) Jumbo bacteriophages: an overview. *Front Microbiol* 8: 403. https://doi.org/10.3389/fmicb.2017.00403
2. Harding KR, Kyte N, Fineran PC (2023) Jumbo phages. *Curr Biol* 33: R750–R751. https://doi.org/10.1016/j.cub.2023.05.056
3. Laughlin TG, Deep A, Prichard AM, et al. (2022) Architecture and self-assembly of the jumbo bacteriophage nuclear shell. *Nature* 608: 429–435. https://doi.org/10.1038/s41586-022-05013-4
4. Kraemer JA, Erb ML, Waddling CA, et al. (2012) A phage tubulin assembles dynamic filaments by an atypical mechanism to center viral DNA within the host cell. *Cell* 149: 1488–1499. https://doi.org/10.1016/j.cell.2012.04.034
5. Thomas JA, Weintraub ST, Wu W, et al. (2012) Extensive proteolysis of head and inner body proteins by a morphogenetic protease in the giant *Pseudomonas aeruginosa* phage φKZ. *Mol Microbiol* 84: 324–339. https://doi.org/10.1111/j.1365-2958.2012.08025.x
6. Lecoutere E, Ceyssens P, Miroshnikov KA, et al. (2009) Identification and comparative analysis of the structural proteomes of ϕKZ and EL, two giant *Pseudomonas aeruginosa* bacteriophages. *Proteomics* 9: 3215–3219. https://doi.org/10.1002/pmic.200800727
7. Sokolova ML, Misovetc I, V Severinov K (2020) Multisubunit RNA polymerases of jumbo bacteriophages. *Viruses* 12: 1064. https://doi.org/10.3390/v12101064
8. De Martín Garrido N, Chen C-S, Ramlaul K, et al. (2024) Structure of the bacteriophage PhiKZ non-virion RNA polymerase transcribing from its promoter p119L. *J Mol Biol* 436: 168713. https://doi.org/10.1016/j.jmb.2024.168713
9. Ceyssens P-J, Minakhin L, Van Den Bossche A, et al. (2014) Development of giant bacteriophage ϕKZ is independent of the host transcription apparatus. *J Virol* 88: 10501–10510. https://doi.org/10.1128/jvi.01347-14
10. Cui J, Schlub TE, Holmes EC (2014) An allometric relationship between the genome length and virion volume of viruses. *J Virol* 88: 6403–6410. https://doi.org/10.1128/jvi.00362-14
11. Ouyang R, Costa AR, Cassidy CK, et al. (2022) High-resolution reconstruction of a Jumbo-bacteriophage infecting capsulated bacteria using hyperbranched tail fibers. *Nat Commun* 13: 7241. https://doi.org/10.1038/s41467-022-34972-5
12. Yang Y, Shao Q, Guo M, et al. (2024) Capsid structure of bacteriophage ΦKZ provides insights into assembly and stabilization of jumbo phages. *Nat Commun* 15: 6551. https://doi.org/10.1038/s41467-024-50811-1
13. Hua J, Huet A, Lopez CA, et al. (2017) Capsids and genomes of jumbo-ssized bacteriophages reveal the evolutionary reach of the HK97 fold. *mBio* 8: e01579-17. https://doi.org/10.1128/mbio.01579-17
14. Neumann E, Kawasaki T, Effantin G, et al. (2020) 3D structure of three jumbo phage heads. *J Gen Virol* 101: 1219–1226. https://doi.org/10.1099/jgv.0.001487

15. González B, Monroe L, Li K, et al. (2020) Phage G structure at 6.1 Å resolution, condensed DNA, and host identity revision to a *Lysinibacillus*. *J Mol Biol* 432: 4139–4153. https://doi.org/10.1016/j.jmb.2020.05.016
16. Krylov VN, Smirnova TA, Minenkova IB, et al. (1984) *Pseudomonas* bacteriophage contains an inner body in its capsid. *Can J Microbiol* 30: 758–762. https://doi.org/10.1139/m84-116
17. Wu W, Thomas JA, Cheng N, et al. (2012) Bubblegrams reveal the inner bbody of bacteriophage ϕKZ. *Science* 335: 182–182. https://doi.org/10.1126/science.1214120
18. Sokolova OS, Shaburova OV, Pechnikova EV, et al. (2014) Genome packaging in EL and Lin68, two giant phiKZ-like bacteriophages of P. aeruginosa. *Virology* 468–470: 472–478. https://doi.org/10.1016/j.virol.2014.09.002
19. Chaikeeratisak V, Khanna K, Nguyen KT, et al. (2022) Subcellular organization of viral particles during maturation of nucleus-forming jumbo phage. *Sci Adv* 8: eabj9670. https://doi.org/10.1126/sciadv.abj9670
20. Nichiporenko A, Antonova D, Kurdyumova I, et al. (2024) Assembly of phiKZ bacteriophage Inner Body during infection. *Biochem Bioph Res Co* 693: 149372. https://doi.org/10.1016/j.bbrc.2023.149372
21. Antonova D, Nichiporenko A, Sobinina M, et al. (2024) Genomic transfer via membrane vesicle: a strategy of giant phage phiKZ for early infection. *J Virol* e00205-24. https://doi.org/10.1128/jvi.00205-24
22. Danilova YA, Belousova VV, Moiseenko AV, et al. (2020) Maturation of pseudo-nucleus compartment in P. aeruginosa, infected with giant phiKZ phage. *Viruses* 12: 1197. https://doi.org/10.3390/v12101197
23. Thomas JA, Black LW (2013) Mutational analysis of the *Pseudomonas* aeruginosa myovirus ϕKZ morphogenetic protease gp175. *J Virol* 87: 8713–8725. https://dx.doi.org/10.1128/jvi.01008-13
24. Fossati A, Mozumdar D, Kokontis C, et al. (2023) Next-generation proteomics for quantitative jumbophage-bacteria interaction mapping. *Nat Commun* 14: 5156. https://doi.org/10.1038/s41467-023-40724-w
25. Cheng N, Wu W, Watts NR, et al. (2014) Exploiting radiation damage to map proteins in nucleoprotein complexes: the internal structure of bacteriophage T7. *J Struct Biol* 185: 250–256. https://doi.org/10.1016/j.jsb.2013.12.004
26. Wu W, Leavitt JC, Cheng N, et al. (2016) Localization of the houdinisome (ejection proteins) inside the bacteriophage P22 Virion by bubblegram imaging. *mBio* 7: e01152-16. https://doi.org/10.1128/mBio.01152-16
27. Glaeser RM (2016) Specimen behavior in the electron beam, *Methods in Enzymology*, Elsevier, 19–50. https://doi.org/10.1016/bs.mie.2016.04.010
28. Wu W, Cheng N, Black L, et al. (2020) Biphasic packing of DNA and internal proteins in bacteriophage T4 heads revealed by bubblegram imaging. *Viruses* 12: 1282. https://doi.org/10.3390/v12111282
29. Zheng J, Xiao H, Pang H, et al. (2025) Conformational changes in and translocation of small proteins: insights into the ejection mechanism of podophages. *J Virol* 99: e01249-24. https://doi.org/10.1128/jvi.01249-24
30. Iglesias SM, Lokareddy RK, Yang R, et al. (2023) Molecular architecture of *Salmonella* typhimurium virus P22 genome ejection machinery. *J Mol Biol* 435: 168365. https://doi.org/10.1016/j.jmb.2023.168365

31. McNulty R, Cardone G, Gilcrease EB, et al. (2018) Cryo-EM elucidation of the structure of bacteriophage P22 virions after genome release. *Biophys J* 114: 1295–1301. https://doi.org/10.1016/j.bpj.2018.01.026
32. Punjani A, Rubinstein JL, Fleet DJ, et al. (2017) cryoSPARC: algorithms for rapid unsupervised cryo-EM structure determination. *Nat Methods* 14: 290–296. https://doi.org/10.1038/nmeth.4169
33. Meng EC, Goddard TD, Pettersen EF, et al. (2023) UCSF CHIMERAX : tools for structure building and analysis. *Protein Sci* 32: e4792. https://doi.org/10.1002/pro.4792
34. Nishimura Y, Yamada K, Okazaki Y, et al. (2024) DiGAlign: versatile and interactive visualization of sequence alignment for comparative genomics. *Microb Environ* 39: ME23061. https://doi.org/10.1264/jsme2.me23061
35. Effantin G, Hamasaki R, Kawasaki T, et al. (2013) Cryo-electron microscopy three-dimensional structure of the jumbo phage ΦRSL1 infecting the phytopathogen *Ralstonia solanacearum*. *Structure* 21: 298–305. https://doi.org/10.1016/j.str.2012.12.017
36. Krylov VN, Zhazykov IZ (1978) Pseudomonas bacteriophage phiKZ-possible model for studying the genetic control of morphogenesi. *Genetika* 14: 678–685.
37. Plotnikova TG, Dzhusupova AB, Khrenova EA, et al. (1982) Genetic and phenogenetic study of the ts-mutant group of *Pseudomonas aeruginosa* PA01 phage phi KZ. *Genetika* 18: 1793–1798.
38. Matsko N (2001) Atomic force microscopy analysis of bacteriophages PhiKZ and T4. *J Electron Microsc* 50: 417–422. https://doi.org/10.1093/jmicro/50.5.417
39. Huiskonen JT (2018) Image processing for cryogenic transmission electron microscopy of symmetry-mismatched complexes. *Bioscience Rep* 38: BSR20170203. https://doi.org/10.1042/BSR20170203

AIMS Press